Nanomaterials and Polymers Innovations Vol. 1, No. 1 (2025); 19-31
ISSN: 3102-0798 (Online). Available online at www.nepalpolymer.org

Original research paper

Cellulose Nanocrystals-Based Nanocomposites for Magnetic Solid-Phase Extraction of PAHs from Water Samples

Luciana Costa dos Reis[1], Isabella Karoline Ribeiro Dias[2], Valdeir Arantes[2], Elizabete Fernandes Lucas[1,3*], Bluma Guenther Soares[1,3]

[1]*Universidade Federal do Rio de Janeiro, Instituto de Macromoléculas Professora Eloisa Mano, Rio de Janeiro, Brazil; elucas@ima.ufrj.br*

[2]*Universidade de São Paulo, Escola de Engenharia de Lorena, Departamento de Biotecnologia Industrial/DEBIQ, Lorena, Brazil*

[3]*Universidade Federal do Rio de Janeiro, Programa de Engenharia Metalúrgica e de Materiais/COPPE, Rio de Janeiro, Brazil*

ORCID: 0000-0002-9454-9517 (EFL), ORCID: 0000-0002-1273-7574 (BGS), and ORCID: 0000-0001-9461-7914 (LCdR)

Abstract: An eco-friendly magnetic nanocomposite based on cellulose nanocrystals (CNCs) was synthesized through a rapid and straightforward method, utilizing electrostatic interactions between Fe_2O_3 nanoparticles and CNCs (CNCs/Fe_2O_3). These nanocomposites were characterized by scanning electron microscopy-energy dispersive X-ray spectrometry (SEM-EDX) and Fourier transform infrared spectroscopy (FTIR). These hybrid materials were effectively employed for the adsorption of three polycyclic aromatic hydrocarbons (PAHs), naphthalene, fluorene and pyrene from water samples, using magnetic solid-phase extraction (MSPE) as the preconcentration technique. Among the tested formulations, the CNCs/Fe_2O_3 with a mass ratio of 3/1 demonstrated the highest adsorption capacity for all three PAHs. The following order was observed for the extraction efficiency: pyrene > fluorene > naphthalene. MSPE process was optimized using a Plackett–Burman design to identify the most influential experimental parameters.

Keywords: cellulose nanocrystals; polycyclic aromatic hydrocarbons; preconcentration; sorbent

शोधसार: प्रस्तुत अनुसन्धानमा फेरिक अक्साइड र सेलुलोजका नानोकणिकाहरु बिचको स्थिर विद्युतिय अन्तरक्रियाको उपयोग गरेर चुम्बकीय गुणयुक्त वातावरणमैत्री नानोसमिश्रण संश्लेषण गर्ने छिटो र सरल विधिको अध्ययन गरिएको थियो । यसरी तयार गरिएका समिश्रणहरूको अनेकन विशेषताहरु निर्धारण गर्नका लागि स्क्यानिङ इलेक्ट्रोन माइक्रोस्कोपी–इनर्जी डिस्पर्सिभ एक्स-रे स्पेक्ट्रोमेट्री (SEM-EDX) र फोरिएर ट्रान्सफर्म इन्फ्रारेड स्पेक्ट्रोस्कोपी जस्ता उपकरणहरु प्रयोग गरिएका थिए । उक्त समिश्रणहरूलाई *चुम्बकीय ठोस निष्कर्षण प्रविधि* (MSPS) समेत अपनाएर पानीलाई नराम्ररी दुषित गर्ने ३ बिभिन्न प्रकारका पोलिएरोम्याटिक हाइड्रोकार्बनहरू (जस्तैः नाफ्थालिन, फ्लोरिन र पाइरिन) को प्रभावकारी अवशोषणका लागि प्रयोग गरियो । परीक्षण गरिएका नमुनाहरू मध्ये सेलुलोज र फेरिक अक्साइडका नानोकणिकाहरुको मात्रात्मक अनुपात ३:१ रहेको नानोसमिश्रणले देहाय अनुसारको क्रममा सर्वोत्तम अवशोषण क्षमता प्रदर्शन गरेको पाईयो: पाइरिन > फ्लोरिन > नाफ्थालिन । निष्कर्षमा दुषित-जल-प्रशोधन प्रयोजनार्थ प्रभावी प्रयोगात्मक सुचकहरूको पहिचान हेतु प्लाकेट्-बर्मन डिजाइनको उपयोग गरी उल्लेखित चुम्बकीय ठोस निष्कर्षण प्रविधिको पनि सुधार गरिएको थियो।

INTRODUCTION

Water is extensively used in the petroleum industry to enhance oil production. The resulting byproduct, known as produced water or oily water, is extracted from the reservoir alongside crude oil. This mixture

Corresponding author, E-mail: *elucas@ima.ufrj.br*

Received: April 25, 2025; Revised: May 11, 2025, Accepted: May 12, 2025; Published: May 19, 2025

comprises formation water (naturally occurring water within the reservoir) and connate water (injected water used to boost oil extraction and maintain the reservoir pressure). Produced water contains elevated level of organic pollutants, notably polycyclic aromatic hydrocarbons (PAHs) (Amakiri et al., 2024). Other prevalent contaminants include BTEX compounds (benzene, toluene, ethylbenzene, xylenes, and phenol), all classified as high-priority chemicals by the EPA (2019) and WHO (2019). Nowadays, global oil production increases to supply energy demand. Consequently, the volume of produced water also escalates. (Amakiri et al., 2022).

PAHs are persistent organic pollutants characterized by two or more condensed aromatic rings. They are hazardous to both the environment and human health, exhibiting carcinogenic, mutagenic, and immunosuppressive properties (EPA, 2019; WHO 2019). The discharge of the produced water into marine environments is a significant source of PAH contamination. Studies have identified and quantified PAHs in oily water samples (Binet et al., 2011; Gabardo et al., 2011; Venkatesan and Wankat, 2017). PAHs present low water solubility, low volatility, and tend to accumulate in organisms and aquatic sediments (Zhang et al., 2016).

Concentrations of PAHs in produced water range from about 0.01 µg L^{-1} to 1512 µg L^{-1}, with naphthalene and fluorene among the most prevalent (**Table 1**) (Pampani and Sydnes, 2013; Petrobras, 2021). Variations in concentration levels are attributed to differences in oil field locations and reservoir characteristics.

Naphthalene is genotoxic and induces tumors in experimental animals (IARC, 1985; IARC, 2012). Additionally, naphthalene irritates human skin and can cause allergic reaction in both humans and animals (IARC, 2012). Fluorene is not classified as a carcinogen; however, studies on oral exposure in humans demonstrated a decrease in red blood cell count, packed cell volume, and hemoglobin levels (EPA, 1990a). Pyrene is not classified as carcinogenic by the EPA (1990b); nevertheless, it is a skin irritant, a suspected mutagen, and a possible tumor-causing agent (EPA, 1990b).

Table 1. Concentration values (µg L^{-1}) of major PAHsin produced water from various marine regions (Pampanim and Sydnes, 2013; PETROBRAS, 2021.

Compound	Great Britain North Sea[a]	Scotian Shelf Canada[a]	North America Gulf of Mexico[a]	Brazil Santos Basin FPSO* Mangaratiba[b]	Brazil Santos Basin FPSO* P-66 Angra dos Reis[b]
Pyrene	0.03 - 1.9	0.36	0.01 - 0.29	0 - 0.40	<0.05 - 0.12
Naphthalene	237 – 394	1512	5.3 - 90.2	17.3 - 33.5	20.2 - 80.3
Fluorene	2.6 - 21.7	13	0.06 - 2.8	1.2 - 1.8	0.80 - 4
Phenanthrene	1.3 - 32.0	4.0	0.11 - 8.8	0 - 7.0	2.7 – 16.5
Anthracene	ND	0.26	0.45	ND	<0.05
Total PAHs	419 - 1559	2148	40 - 600	27.6 - 39	23.8 - 101

[a] (Pampanim and Sydnes, 2013);
[b] (PETROBRAS, 2021).
*Floating Production Storage Offloading Unit

Produced water treatment typically occurs at the oil field surface, utilizing separation tanks, hydrocyclones and floaters units. The disposal process follows the guideline established by CONAMA Resolution 393/2007, which allows for an average concentration of oil and grease up to 29 mg L^{-1}, and a maximum daily limit of 42 mg L^{-1} (CONAMA, 2007; Petrobras, 2022). For marine disposal, the resolution also establishes monitoring of additional parameters, including organic

compounds (PAHs, BTEX, phenols and evaluation of total hydrocarbons) (CONAMA, 2007).

Precisely measuring PAH levels in water samples is crucial to ensure adherence to environmental regulations. This requires effective sample preparation and extraction techniques. The common analytical techniques for PAHs detection include high-performance liquid chromatography (HPLC) with UV-visible or fluorescence detection, gas chromatography-mass spectrometry (GC-MS), and fluorescence spectroscopy (Gratz et al., 2000; Song et al., 2012).

Gabardo et al. collected water samples from Guanabara Bay (Rio de Janeiro, Brazil), storing them in dark containers at temperatures below 5 °C. PAHs were extracted using liquid-liquid extraction with n-hexane and analyzed by UV-fluorescence spectrometry. PAHs concentrations ranged from 0.04 to 24.48 μg L^{-1} (Gabardo et al., 2001).

Delgado et al. collected seawater samples from a Spanish beach near an oil industry and analyzed the presence of PAHs by liquid chromatograph equipped with a scanning fluorescence detector. Subsequent quantification by HPLC allowed the determination of 13 PAHs, with limits of detection up to 23 mg L^{-1} and an average total relative standard deviation (RSD) of 9.2 % (Delgado et al., 2004).

Analyzing PAHs in water requires indirect methods, as direct detection is often challenging due to the complex composition of the produced water. Therefore, the determination of the concentration of each compound requires a sample preparation process, including efficient extraction techniques. One of the miniaturized extraction techniques that has been widely used for the extraction of PAHs is magnetic solid phase extraction (MSPE). This is a miniaturized method that becomes popular for PAH extraction. In MSPE, a magnetic hybrid adsorbent is dispersed in the liquid sample, favoring interaction between the sample and the extracting solid phase (Šafaříková and Šafařík, 1999). The magnetic component allows for easy handling using an external magnetic field (magnet), while the extracting phase adsorbs the target analytes through various chemical interactions (Sasaki and Tanaka, 2011). Selecting appropriate adsorbent materials enhances extraction selectivity and efficiency, and, in some cases, the materials can be reused (Yaping et al., 2014).

The magnetic phase in MSPE technique often consists of iron-based minerals or iron oxides, such as magnetite (Fe_3O_4) or maghemite (γ-Fe_2O_3). The extracting phase may include organic and inorganic compounds forming composites (Yang et al., 2019). Some of them include carbon nanotubes integrated into iron-based metal-organic frameworks (Yang et al., 2022), or graphene oxide modified with polyaniline (Manousi et al., 2021) among others. The main adsorption mechanism for PAHs is based on π-π interactions between the aromatic structures and those of the adsorbent material. Consequently, an ideal solid adsorbent should possess a high surface area and abundant conjugated double bonds (Zhang et al., 2011). Carbon-based materials are commonly used for PAH adsorption due to their high specific surface area and presence of π orbitals (Kong et al., 2011).

The cellulose nanocrystals (CNCs) are renewable nanomaterial that serve as green alternatives to traditional sorbents for the sample preparation techniques due to their biocompatibility, biodegradability, and chemical stability (Dufresne, 2013). CNCs exhibit strong intermolecular and intramolecular hydrogen bonds enhancing their reactivity (Ruiz-Palomero et al., 2017). Additionally, CNCs can be easily coupled with magnetic nanoparticles to form magnetic nanocomposites, offering efficient and economical options for preconcentration, clean-up and extraction operations. These composites are hydrophilic with controlled retention of the target analytes and can be rapidly recovered using a magnet (Abujaber et al., 2019).

The multifunctional properties of the nanocellulose-based offer significant advantages in the application of adsorbent composite materials (Soares et al., 2024). These materials have garnered attention in the treatment of heavy metal wastewater due to their increased number of adsorption active sites and greater biocompatibility (Habibi, 2014; Bhatnagar et al., 2015). These inherent qualities make it suitable as a material for oil-water separation. Bio-based nanocellulose materials are also effective in the adsorption and degradation of organic pollutants due to their excellent physicochemical properties (Aoudi et al., 2022). Nanocellulose can remove several pollutants from water such as heavy metal ions, nitrates, phosphates, dyes, oils, pesticides and

pharmaceuticals due to the possibility of modifying their hydroxyl groups (Mautner, 2020).

In this work, cellulose nanocrystals (CNCs), previously produced by an enzyme-mediated method (Arantes et al., 2020a), an eco-friendly and low-cost method compared to traditional processes, was used to synthesize a magnetic nanocomposite. In aqueous solution, the CNCs are dispersed and negatively charged, allowing the formation of a nanocomposite through electrostatic attraction with positively charged iron oxide (Fe_2O_3) magnetic nanoparticles. The magnetic composite was employed as a sorbent in the MSPE technique. This technique, using the newly produced CNCs/Fe_2O_3 nanocomposite, enabled the isolation and preconcentration of naphthalene, fluorene and pyrene in water. These PAHs were selected due to their high abundance in the produced water by the petroleum industry.

MATERIALS AND METHODS

Materials

The CNCs sample used in the synthesis of the magnetic nanocomposite was previously obtained by enzyme-mediated isolation from a Eucalyptus bleached Kraft pulp according to the literature (Arantes et al., 2020a; 2020b) and dispersed in water at a concentration of 0.3 wt%. $FeCl_3$-$6H_2O$ and $FeSO_4$-$7H_2O$, as well as naphthalene, fluorene and pyrene (analytical standard) were purchased from Sigma-Aldrich (St. Louis, MO, USA), NaOH (97 % purity, pellets) and HNO_3 65 % were acquire from Vetec Química Fina (Xerém, RJ, Brazil). Distilled water (pH 5) was prepared on a water purification system (Q341) supplied by Quimis. The organic solvents (acetonitrile, hexane, methanol, dichloromethane and pentane) were obtained from Labsynth (Diadema, SP, Brazil). Stock standard solutions of each PAH (100 mg L^{-1}) were prepared in acetonitrile. Working solution (10 mg L^{-1}) of the three PAHs was prepared daily by diluting the stock standard solutions with distilled water. All solutions were stored protected from the light at 4 °C.

Fe_2O_3 synthesis

The magnetic component of nanocomposite, iron oxide (Fe_2O_3), was synthesized exactly according to the literature (Fernández and Vidal, 2016). Briefly, 0.780 g of $FeCl_3.6H_2O$ and 0.400 g of $FeSO_4.7H_2O$ were dissolved in 250 mL of distilled water. Then, a 5 M NaOH solution was added dropwise under constant stirring to precipitate the iron oxide. The resulting Fe_2O_3 nanoparticles were washed with distilled water until the pH of the washings reached 7, separated from non-magnetic nanoparticles using a neodymium magnet, and dried at 60 °C overnight.

Synthesis of CNCs/Fe_2O_3 nanocomposite

The CNCs/Fe_2O_3 nanocomposites were synthesized based on a method described by Costa dos Reis et al. (2017). A dispersion of CNC in distilled water (1 mg mL^{-1}) was prepared using ultrasound energy (Fisherbrand CPX3800) for 1 h. CNC possess hydroxyl (-OH) groups on their surface, which, upon ultrasound treatment, loose hydrogen ion rendering the surface negatively charged. Separately, Fe_2O_3 nanoparticles were dispersed in 1M HNO_3 and sonicated for 30 min to achieve a concentration of 150 mg mL^{-1}. This process produces a positive charge in their surface. The two dispersions were then mixed, and the pH of the mixture (CNCs solution + Fe_2O_3 solution) was adjusted to 2. The mixture was vigorously stirred for 1 h, allowing the electrostatic self-assembly occur, forming the CNCs/Fe_2O_3 nanocomposite. The nanocomposite was separated using an external magnetic field and dried in an oven at 60 °C overnight. CNCs/Fe_2O_3 ratios of 1/1 and 3/1 (w/w) were prepared. **Figure 1** illustrates the synthesis procedure.

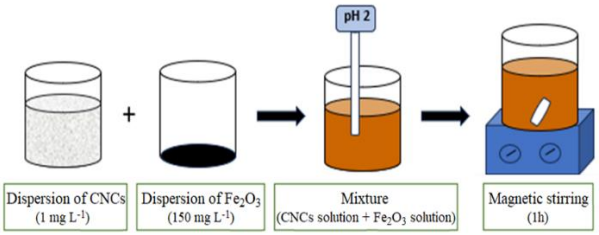

Figure 1. Synthesis procedure of CNCs/Fe_2O_3 nanocomposite.

Magnetic solid-phase extraction procedure

The CNCs/Fe_2O_3 nanocomposite developed in this study was used as adsorbent in the aqueous sample pretreatment technique known as MSPE. The studies employed fluorene, pyrene and naphthalene as model analytes. Standard solutions of each PAH were prepared in acetonitrile at concentrations of 100 mg L^{-1}. A working aqueous solution containing 10 mg L^{-1} of each PAH was then prepared by

diluting the standard solutions. The MSPE procedure is illustrated in **Figure 2**.

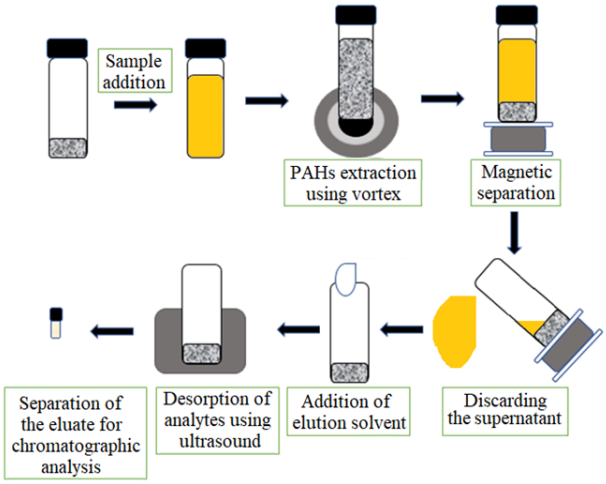

Figure 2. MSPE procedure for the preconcentration of PAHs (prepared by the author).

In the MSPE procedure, 20 mg of CNCs/Fe_2O_3 nanocomposite (1/1 and 3/1 mass ratios) were mixed with 10 mL of work solution. The mixture was agitated for 10 min and the vial was placed on a neodymium magnet to separate the nanocomposite, which was deposited at the bottom due to magnetic attraction. The liquid phase was discarded.

For the adsorption of PAHs, the nanoparticles of the nanocomposite were treated with 0.5 mL of hexane (eluent) in an ultrasonic bath for 5 min. The eluate was separated from the nanocomposite using magnetic separation and transferred to a chromatography vial for analysis. Acetonitrile/dichloromethane mixture was also used as eluent.

Gas chromatography- Flame ionization detection (GC-FID) analysis

Eluates obtained from the MSPE procedure, along with standard solutions containing the three PAHs, were analyzed using a gas chromatograph (Shimadzu, model QP2010) equipped with a split/splitless automatic injector and a flame ionization detector, Japan. A capillary column RTX-5 (diphenyl dimethyl polysiloxane, 30 m x 0.25 mm ID, 0.25 µm film thickness) was used. The injector temperature was set at 250 °C and the injection volume was 1 µL in splitless mode. The oven temperature program was as follows: initially set at 50 °C (held for 3 min), then increased at 30 °C/min to 300 °C (held for 4 min). Helium (99.999 %) at a flow rate of 30 mL min^{-1} was used as carrier gas. The detector temperature was set at 320 °C.

SEM-EDX analysis

The morphology of the nanoparticles was examined using scanning electron microscopy (SEM) with a TESCAN VEGA III microscope (Czech Republic), operating at 20 kV. Elemental analysis was performed with an energy dispersive X-ray (EDX) detector from Bruker Nano GmbH (Germany), model XFlash 630M. EDX microanalysis is an elemental analysis technique associated with SEM, based on the generation of characteristic X-rays that reveals the presence of elements in the sample.

Particle size analysis

Particle size and particle size distribution was determined using a laser diffraction particle size analyzer (Mastersizer 3000, Malvern Instruments). The analyzer employs two light sources: red (632.8 nm) and blue (470 nm), allowing measurement of the hydrodynamic diameter of particles in the range of 10 nm to 3500 µm. Analyses were conducted at low obscuration (0.5 – 4 %), with a stir rotation speed fixed at 3500 rpm, without sonication. The input parameters were manually set to assume a non-spherical particle model, and the refractive index for cellulose (1.4683) was used (Sultanova et al., 2013). Each analysis was performed in duplicate, with three runs, each comprising five successive laser diffraction measurements, totaling 15 readings per sample. Before each analysis, the dispersion unit was automatically cleaned three times with ultrapure water.

Changes in particle size distribution were evaluated by comparing the reduction in peak height after enzymatic treatment to that of the untreated reference pulp (BEKP). The particle size metrics, Dx (10), Dx (50) Dx (90), represent the diameters below which 10 %, 50 % and 90 % of the particles fall, respectively, indicating the distribution of particle sizes within the sample.

FTIR analysis

Fourier Transform Infrared Spectroscopy (FTIR) was employed to investigate the chemical structure of the samples. Measurements were performed using a Perkin Elmer FTIR Spectrometer (Frontier, Perkin Elmer, UK), operating with scanning in the

range of 400 to 4000 cm^{-1}, with a resolution of 1 cm^{-1}, and 32 scans.

Data processing

The optimization of the MSPE conditions was carried out using NEMRODW® statistical software (version 2007/2010) ("New Efficient Methodology for Research using Optimal Design") developed by LPRAI (Marseille, France). This software facilitated the construction of experimental design matrices and the analysis of response variables. The peak areas from chromatographic analysis of each PAH were used as the response function to evaluate extraction efficiency. All experimental procedures were conducted in compliance with laboratory safety protocols and adhered to principles of good scientific practice and research integrity.

RESULTS AND DISCUSSION

Characterization of CNCs/Fe_2O_3 nanocomposites

Figure 3 shows the FTIR spectra of CNCs, Fe_2O_3, and the CNCs/Fe_2O_3 nanocomposites. The CNCs spectrum exhibits a broad absorption band centered around 3420 cm^{-1}, which is attributed to the O-H stretching vibrations of hydroxyl groups in cellulose and absorbed water (Maria Claro et al., 2024). A distinct peak at approximately 2900 cm^{-1} corresponds to the C-H stretching vibration. The absorption band observed near 1640 cm^{-1} is also indicative of absorbed water in the sample (Maria Claro et al., 2024). Additionally, the band at 1200 - 1000 cm^{-1} region is associated with C-O stretching vibrations, characteristic of the cellulose backbone. In the Fe_2O_3 spectrum, a broad band around 3400 cm^{-1} is attributed to O-H stretching vibrations, while a small peak at 1640 cm^{-1} confirms the presence of absorbed water. A prominent absorption band at around 630 cm^{-1} is assigned to the Fe-O stretching vibration, in agreement with previously reported results (Farahmandjou and Soflaee, 2015). The CNCs/Fe_2O_3 nanocomposite spectrum displays key absorption features: a band at 1640 cm^{-1} consistent with absorbed water, a peak around 1390 cm^{-1} corresponding to C–H bending vibrations, and a band near 607 cm^{-1} attributed to Fe–O bond stretching. The overall spectral profile of the nanocomposite closely resembles that of the CNCs spectrum, which can be explained by the high proportion of CNCs in the composite (3/1 w/w).

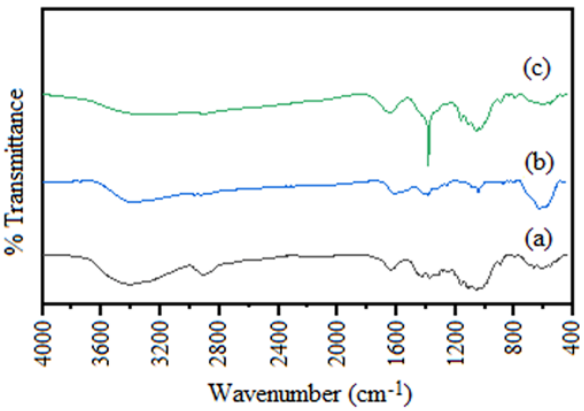

Figure 3. FTIR spectra of (**a**) CNCs, (**b**) Fe_2O_3 and (**c**) CNCs/Fe_2O_3 nanocomposite.

Figure 4 exhibits the SEM micrographs and the corresponding EDX analysis of CNCs, Fe_2O_3 and the CNCs/Fe_2O_3 (3/1) nanocomposite. The Fe_2O_3 nanoparticles appear as irregularly shaped agglomerates (**Figure 4a**) (Costa dos Reis et al., 2017). EDX analysis confirms the presence of iron (58.23 %) and oxygen (36.01 %), consistent with iron oxide composition. The SEM image of the CNCs (**Figure 4b**) reveals sheets-like structures, which contribute to a high surface area, advantageous for extraction purpose. The corresponding EDX spectrum (**Figure 4e**) indicates a high carbon content (63.44 %), followed by oxygen (33.55 %). A small amount of iron detected in the CNCs sample is likely due to contamination of CNCs during the enzymatic hydrolysis of eucalyptus Kraft pulp.

Figure 4c shows SEM image of the CNCs/Fe_2O_3 (3/1) nanocomposite. The image indicates that the smaller Fe_2O_3 nanoparticles are anchored as discrete clusters on the surface of the CNCs sheets. This morphology is attributed to electrostatic self-assembly (Han et al., 2012; Costa dos Reis, 2017), driven by the interaction between the positively charged Fe_2O_3 surface and the negatively charged CNCs in aqueous solution. As expected, the quantity of Fe_2O_3 in the particle is virtually lower than that of CNCs, reflecting the 3/1 (w/w) composition. The EDX spectrum of the nanocomposite (**Figure 2f**) shows a predominant carbon signal (27.41 %) from the nanocellulose matrix, along with oxygen (22.92 %) from both CNCs and Fe_2O_3 , and iron (12.08 %), confirming the successful incorporation of Fe_2O_3 into the nanocomposite.

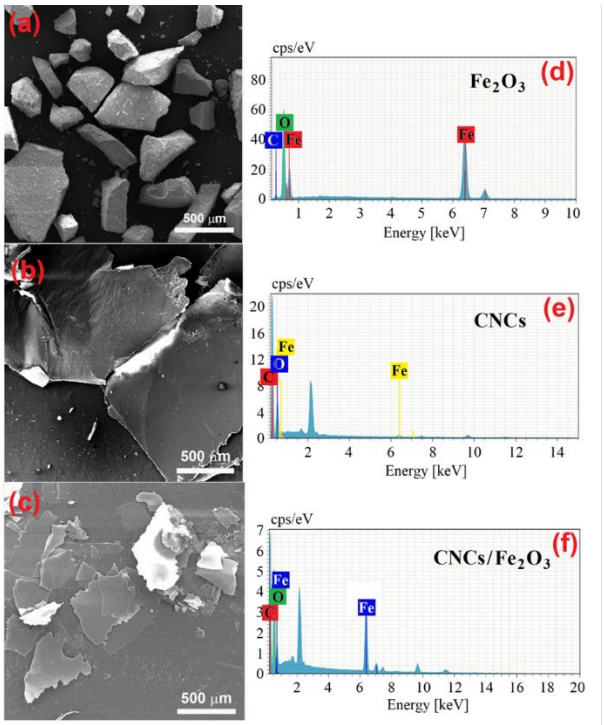

Figure 4. SEM images and EDX spectra of (**a,d**) Fe_2O_3 (**b,e**) CNCs and (**c,f**) CNCs/Fe_2O_3 nanocomposite.

Figure 5 illustrates the particle distribution of Fe_2O_3, CNCs and CNCs/Fe_2O_3 (3/1) nanocomposite. According to the results, Fe_2O_3 nanoparticles presented the average size of 0.46 µm, CNCs nanoparticles and CNCs/Fe_2O_3 (3/1) nanocomposite particles presented the average size of 0.49 µm and 0.89 µm, respectively. These results suggest that Fe_2O_3 nanoparticles were anchored as clusters onto the surface of the CNCs nanoparticles. The particle size of the CNCs/Fe_2O_3 (3/1) nanocomposite reduced drastically (0.89 µm) in comparison to Fe_2O_3 and CNCs. The decrease in size could be attributed to the breakage of CNCs particles during the formation of the nanocomposite carried out under vigorous stirring of the mixture of Fe_2O_3 and CNCs solutions.

Evaluation of the nanocomposite's ability to adsorb PAH

Preliminary investigations into the adsorption performance of the CNCs/Fe_2O_3 nanocomposite were conducted by varying the CNCs/Fe_2O_3 mass ratio. The adsorption efficiency was assessed based on the area of the chromatographic peak, since it is proportional to the concentrations of the analyte. The preconcentration factor (PF) was calculated as the ratio *Ae/Ao*, where *Ao* and *Ae* represent the chromatographic area of the PAH in the standard solution and in the eluate after the extraction, respectively. Experiments were initially carried out with nanocomposite synthesized at pH 2. Using the CNCs/Fe_2O_3 (1/1) nanocomposite, the PF values obtained for naphthalene, fluorene and pyrene were 0.1, 0.1 and 0.2, respectively. These results suggest that pyrene exhibited the highest affinity for the adsorbent material.

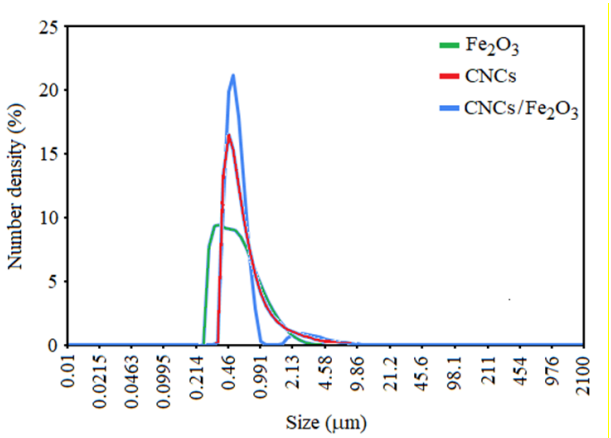

Figure 5. Particle size distribution of Fe_2O_3, CNCs and CNCs/Fe_2O_3 (3/1) nanocomposite.

When the CNCs/Fe_2O_3 mass ratio was increased to 3/1, the PF values improved significantly, reaching 0.5 for naphthalene, 0.87 for fluorene, and 1.64 for pyrene. This indicates that the adsorption efficiency is enhanced by increasing the proportion of CNCs in the composite, because of their high surface area and the electron delocalization (Arantes et al., 2020). These findings support the hypothesis that CNCs serve as the primary adsorptive component in the nanocomposite. Higher CNCs contents were not tested, as an adequate proportion of Fe_2O_3 is necessary to ensure magnetic responsiveness. A significant imbalance between the mass of the adsorbent and the magnetic phase could impair the efficiency of the magnetic solid-phase extraction (MSPE) process.

Based on the improved performance of the CNCs/Fe_2O_3 (3/1) nanocomposite prepared at pH 2, additional batches of this nanocomposite were synthesized at pH 7 and pH 10 to evaluate the influence of the pH during the synthesis on adsorption capacity. **Figure 6** shows the average chromatographic peak areas for naphthalene,

fluorene and pyrene extracted using composites prepared at different pH values.

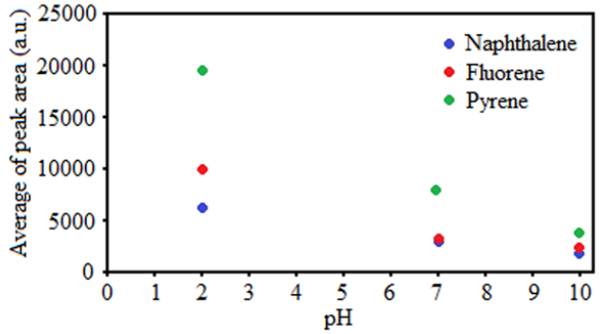

Figure 6. Average chromatographic area for naphthalene, fluorene and pyrene obtained in MSPE´s using nanocomposites synthesized with different pH´s. Synthesis conditions: CNCs/Fe_2O_3 ratio (*w/w*) 3/1 and 1 h of magnetic stirring. Extraction conditions: nanocomposite = 20 mg; standard solution = 20 mL; extraction time = 10 min; eluent = 1 mL; desorption time = 5 min; pH = 5; without NaCl addition.

The highest adsorption capacity was observed with the nanocomposite synthesized at pH 2. This result can be attributed to the electrostatic self-assembly process that occurs between the negatively charged CNCs and the positively charged Fe_2O_3 nanoparticles (Costa dos Reis et al., 2017). At a neutral pH (7), the concentration of H^+ ions is insufficient to fully protonate the Fe_2O_3 particles, reducing the extent of positive charge. Consequently, the electrostatic attraction between Fe_2O_3 and CNCs is weakened, resulting in and inadequately formed composite with fewer magnetic nanoparticles, which negatively affect its adsorption capacity.

In MSPE, nanocomposites with a low proportion of the magnetic phase can present challenges in the separation step. To further optimize the synthesis conditions, nanocomposites with CNCs/Fe_2O_3 mass ratio of 3/1 were prepared at pH 2 with different stirring durations - 1 h and 3 h. These composites were then evaluated for their performance in the preconcentration of naphthalene, fluorene and pyrene. The highest chromatographic peak areas were achieved using the nanocomposite synthesized with 1 h of magnetic stirring.

In conclusion, the optimal synthesis conditions for the CNCs/Fe_2O_3 nanocomposite synthesis were determined to be: CNCs/Fe_2O_3 mass ratio of 3/1, pH 2 and 1 h of magnetic stirring.

Optimization of the MSPE procedure

The optimization study employed a Plackett-Burman design, a two-level fractional factorial design suitable for evaluating up to K = N − 1 variables in N experimental runs, where N is a multiple of 4. This design assumes that interactions between factors are negligible, allowing the main effects to be estimated with a reduced number of experiments (Draper, 1985). In this study, an experimental matrix was constructed to evaluate eight factors, as shown in Table **2**.

Based on the selected experimental design, twelve independent trials were conducted in a random order. The resulting data were analyzed using analysis of variance (ANOVA), and the influence of each factor on the response variables was illustrated using Pareto charts for each PAH, as shown in **Figure 7**. In these charts, the length of each bar represents the magnitude of the factor's effect. Factors with bar extending beyond the reference vertical line are considered statistically significant at a 95 % confidence level.

Additionally, the sign of each event (negative or positive) indicates whether the response decreases or increases, respectively, when the factor changes from its low to high level.

Table 2. Factors and levels of Plackett-Burman design.

Factor	Low level (-1)	High level (+1)
Amount of nanocomposite (mg)	20	40
Vortex extraction time (min)	5	10
Type of eluent	acetonitrile/dichloromethane	hexane
Volume of eluent (mL)	0.5	1
Desorption time in ultrasound (min)	2.5	5
Sample pH	5	12
Volume of sample (mL)	10	20
Ionic strength (% of NaCl)	0	15

In the Pareto charts for all three analytes studied, naphthalene, fluorene, and pyrene, the graphic values for each factor did not exceed the reference line, indicating that none of the evaluated factors were statistically significant for the magnetic solid phase extraction (MSPE) process at the 95 % confidence level. Despite this, the direction of each factor's effect (positive or negative) was used to guide the selection of optimal conditions.

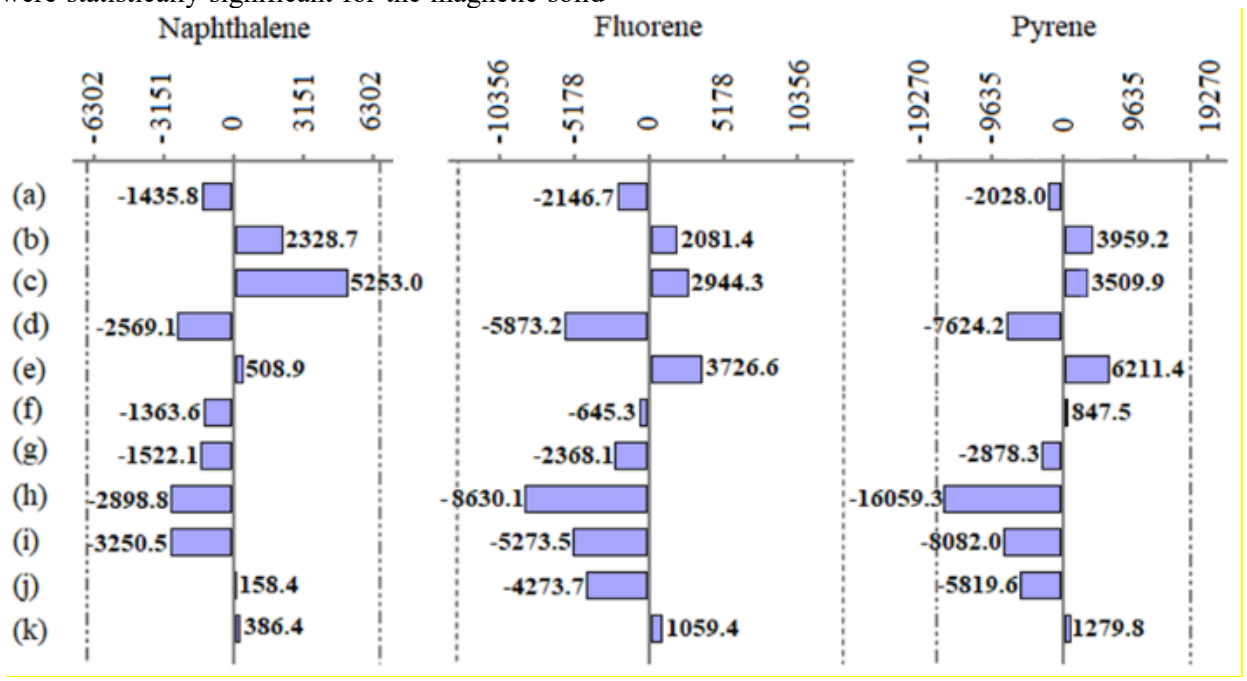

Figure 7. Pareto chart of the Plackett-Burman design for naphthalene, fluorene and pyrene: (**a**) amount of nanocomposite; (**b**) vortex extraction time; (**c**) type of eluent; (**d**) volume of eluent; (**e**) desorption time in ultrasound; (**f**) sample pH; (**g**) volume sample; (**h**) ionic strength; (**i**) ghost 1; (**j**) ghost 2; and (**k**) ghost 3.

For all three PAHs, the following factors showed negative effect on the response: amount of nanocomposite (20 mg), eluent volume (0.5 mL), sample volume (10 mL), and ionic strength (0 % NaCl). Conversely, the following factors had a positive influence: vortex extraction time (10 min), eluent type hexane), and desorption time in an ultrasound (5 min). Sample pH showed a negative effect for naphthalene and fluorene, but a slight positive effect for pyrene. However, due to the minimal impact observed for pyrene, the sample pH was fixed at its lowest tested value (pH 5).

According to the Plackett-Burman experimental design (Draper, 1985), the optimal MSPE conditions for the extraction of naphthalene, fluorene and pyrene were established as follows: 20 mg of CNCs/Fe_2O_3 (3/1) nanocomposite, vortex extraction for 10 min, hexane as the eluent, 0.5 mL of eluent volume, 5 min of ultrasonic desorption time, sample pH of 5, 10 mL of sample volume and no added NaCl.

MSPE under optimal conditions

Three replicate MSPE procedures were performed under the optimal conditions, and the preconcentration factors (PFs) were calculated for each PAH. The PF values were 2 for naphthalene, 4 for fluorene, and 7 for pyrene. These results indicate that the CNCs/Fe_2O_3 (3/1) nanocomposite synthesized under optimal conditions exhibits a greater adsorption - desorption efficiency for pyrene. However, the relatively low PF observed for naphthalene suggests that the current MSPE protocol is suboptimal for its preconcentration. A separate optimization study would be necessary to enhance the extraction efficiency for naphthalene specifically.

CONCLUSION

Based on the findings of this study, the following conclusions can be drawn:

A scalable and efficient method for preparing CNCs/Fe_2O_3 hybrid particles was described, which

relies on the electrostatic attraction between both components.

Magnetic solid-phase extraction (MSPE) was used, to isolate the PAHs from the aqueous phase. Among the composites used, the CNCs/Fe_2O_3 (3/1) exhibited the highest adsorption efficiency. This result suggests that CNCs serves as the primary adsorptive component, while Fe_2O_3 contributes to magnetic separation.

The best extraction performance was observed at pH 2, with the adsorption efficiency following the order: pyrene > fluorene > naphthalene.

To further optimize the extraction process, a Plackett–Burman experimental design was applied to investigate the effects of several variables. The optimal MSPE conditions determined through this design included: 20 mg of CNCs/Fe_2O_3 nanocomposite, 10 minutes of vortex extraction, hexane as the eluent (0.5 mL), 5 minutes of ultrasonic desorption, a sample pH of 5, and a total sample volume of 10 mL.

In conclusion, the CNCs/Fe_2O_3 (3:1) nanocomposite offers a fast, simple, and environmentally sustainable option as an adsorbent in MSPE procedures for the preconcentration of PAHs. It is scalable and eco-friendly synthesis, ease of handling, and effective preconcentration—especially for fluorene and pyrene—underscore its potential in environmental applications, particularly for water quality monitoring and pollutant remediation.

The adsorption-desorption performance demonstrated here may be extended to other PAHs commonly found in produced water.

Availability of Data and Materials

The sets of data generated during and/or analysed during the research work can be available from the corresponding author on logical request.

Funding

The research received grant from: Programa de Recursos Humanos da Agência Nacional do Petróleo, Gás Natural e Biocombustíveis – PRH16.1- ANP; CNPq (305.565/2022-2) and FAPERJ (E-26/204.066/2024).

Author Contributions

Luciana Costa conceived, designed and performed the experiments. Isabella Dias and Valdeir Arantes provided the CNCs (BR 10 2020 025815 0 A2) and provided scientific support on the characteristics and properties of CNCs. Isabella Dias performed particle size and FTIR analyses. Luciana Costa and Bluma Soares performed SEM/EDX analysis. Elizabete Lucas and Bluma Soares analyzed the data. Luciana Costa, Elizabete Lucas and Bluma Soares wrote the paper.

Conflicts of Interest

The authors declare no conflict of interest.

Declarations

No experimental procedure requiring ethical concern was established during this research work. Thus, ethical approval is not required.

Acknowledgments

The authors thank the financial support from "Programa de Recursos Humanos da Agência Nacional do Petróleo, Gás Natural e Biocombustíveis – PRH16.1- ANP". Elizabete Lucas thank the Brazilian Agencies: CAPES, CNPq (305.565/2022-2) and FAPERJ (E-26/204.066/2024). Bárbara Pereira, technician of the "Laboratory of Applied Bionanotechnology of the Department of Biotechnology in the Engineering School of Lorena" (Lorena, São Paulo, Brasil).

REFERENCES

Amakiri KT, Ogolo NA, -Dimakis AA, Albert O. Produced water treatment by semi-continuous sequential bioreactor and microalgae photobioreactor. Bioresources and Bioprocessing. 2024 Jun 8:87-95. DOI: https://doi.org/10.1186/s40643-024-00775-3

Amakiri KT, Canon AR, Molinari M, Angelis-Dimakis A. Review of oilfield produced water treatment technologies. Chemosphere. 2022 Jul 298:1-20. DOI: https://doi.org/10.1016/j.chemosphere.2022.134064

Abujaber F, Jiménez-Moreno M, Bernardo FJG, Martín-Doimeadios RCR. Simultaneous extraction and preconcentration of monomethylmercury and inorganic mercury using magnetic cellulose nanoparticles. Microchimica Acta. 2019 Jun 186:400. DOI: https://doi.org/10.1007/s00604-019-3492-8

Aoudi B, Boluk Y, Gamal El-Din M. Recent advances and future perspective on nanocellulose-based materials in diverse water treatment applications. Science of the Total Environment. 2022 Oct 843:156903. DOI: https://doi.org/10.1016/j.scitotenv.2022.156903

Arantes V, Dias IKR, Berto GL, Pereira B, Marotti BS, Nogueira CFO. The current status of the enzyme-mediated isolation and functionalization of nanocelluloses: production, properties, techno-economics, and opportunities. Cellulose. 2020 Jul 27:10571-10630. (a). DOI: https://doi.org/10.1007/s10570-020-03332-1

Arantes V, Dias IKR, Santos JC, Hilares RT. Processo de Preparação de Soluções Estáveis de Nanocristais de Celulose por Meio de Pós-tratamento por Cavitação Hidrodinâmica. Holder: Universidade de São Paulo. BR 10 2020 025815 0 A2. Deposit: Dec 17, (2020). Concession: Jun 28, 2022. Int. Ci. D21C 9/00 (2006.01), D21C 3/00 (2006.01). (b).

Bhatnagar A, Sillanpaa M, Witek-Krowiak A. Agricultural waste peels as versatile biomass for water purification – A review. Chemical Engineering Journal. Jun 2015 270:244-271. DOI: https://doi.org/10.1016/j.cej.2015.01.135

Binet MT, Stauber JL, Winton T. The Effect of Storage Conditions on Produced Water Chemistry and Toxicity. In Lee, K., Neff, J. (eds) Produced Water 2011. Springer, New York. DOI: https://doi.org/10.1007/978-1-4614-0046-2_7

CONAMA RESOLUTION 393, August 8, 2007; "Establishes provisions for the continuous release of processed water or water produced on oil and natural gas sea platforms and makes other provisions; Published in Official Gazette 153 on August 9, Section 1, pages 72-73.

Costa dos Reis L, Vidal L, Canals A. Graphene oxide/Fe_3O_4 as sorbent for magnetic solid-phase extraction coupled with liquid chromatography to determine 2,4,6-trinitrotoluene in water samples. Analytical and Bioanalytical Chemistry. 2017 Feb 409:2665-2674. DOI: https://doi.org/10.1007/s00216-017-0211-3

Delgado B, Pino V, Ayala JH, González V, Afonso AM. Nonionic surfactant mixtures: a new cloud-point extraction approach for the determination of PAHs in seawater using HPLC with fluorimetric detection. Analytica Chimica Acta. 2004 Aug 518:165-172. DOI: https://doi.org/10.1016/j.aca.2004.05.005

Draper NR. Plackett and Burman designs. In: Kotz S, Johnson L, editors. Encyclopedia of Statistical Sciences 1985. New York: John Wiley & Sons.

Dufresne A. Nanocellulose: a new ageless bionanomaterial. Materials Today. 2013 Jun 16:220-227. DOI: https://doi.org/10.1016/j.mattod.2013.06.004

EPA "Industrial Wastewater Treatment Technology". United States Environmental Protection Agency. 2019 [12/05/2025] Available from: Final Report: Oil and Gas Extraction Wastewater Management | US EPA

EPA, "IRIS Assessment". United States Environmental Protection Agency. 1990 [12/05/2015] Available from: Fluorene CASRN 86-73-7 | IRIS | US EPA, ORD (12/05/2025) (a).

EPA, "IRIS Assessment". United States Environmental Protection Agency. 1990 [12/05/2025] Available from: Pyrene (CASRN 129-00-0) | IRIS | US EPA (b).

Farahmandjou M, Soflaee F. Synthesis and characterization of α-Fe_2O_3 nanoparticles by simple co-precipitation method. Physical Chemistry Research. 2015 Sep 3:191-196. DOI: https://doi.org/10.22036/pcr.2015.9193

Fernández E, Vidal L, Canals A. Zeolite/iron oxide composite as sorbent for magnetic solid-phase extraction of benzene, toluene, ethylbenzene and xylenes from water samples prior to gas chromatography/mass spectrometry. Journal of Chromatography A. 2016 Aug 1458:18-24. DOI: https://doi.org/10.1016/j.chroma.2016.06.049

Gabardo IT, Meniconi MFG, Falcão LV, Vital NAA, Pereira RCL, Carreira RS. Hydrocarbon and Ecotoxicity in seawater and sediment samples of Guanabara Bay after the oil spill. International Oil Spill Conference Proceedings 2001. 2:941-950. DOI: https://doi.org/10.7901/2169-3358-2001-2-941

Gabardo IT, Platte EB, Araujo AS, Pulgatti FH, Evaluation of Produced Water from Brazilian Offshore Platforms. In: Lee, K., Neff, J. (eds) Produced Water 2011. Springer, New York. DOI: https://doi.org/10.1007/978-1-4614-0046-2_3

Gratz LD, Bagley ST, Leddy DG, Johnson JH, Chiu C, Stommel P. Interlaboratory Comparison of HPLC-Fluorescence Detection and GC/MS: Analysis of PAH Compounds Present in Diesel Exhaust. Journal of Hazardous Materials. 2000 May 74:37-46. DOI: https://doi.org/10.1016/s0304-3894(99)00197-1

Habibi Y. Key advances in the chemical modification of nanocelluloses. Chemical Society Reviews. 2014 43:1519-1542. DOI: https://doi.org/10.1039/C3CS60204D
Han Q, Wang Z, Xia J, Chen S, Zhang X, Ding M. Facile and tunable fabrication of Fe_3O_4/graphene oxide nanocomposites and their application in the magnetic solid-phase extraction of polycyclic aromatic hydrocarbons from environmental water samples. Talanta. 2012 Nov 101:388–395. DOI: https://doi.org/10.1016/j.talanta.2012.09.046
IARC, International Agency for Research on Cancer 1985 [12/05/2025] Available from: http://monographs.iarc.fr/ENG/Monographs/vol1-42/mono35.pdf.
IARC, International Agency for Research on Cancer 2012 [12/05/2025] Available from: http://monographs.iarc.fr/ENG/Monographs/vol100F/mono100F.pdf.
Kong H, He J, Gao Y, Han J, Zhu X. Removal of Polycyclic Aromatic Hydrocarbons from Aqueous Solution on Soybean Stalk–based Carbon. Journal of Environmental Quality. 2011 Nov. 40:1737-1744. DOI: https://doi.org/10.2134/jeq2010.0343
Manousi N, Deliyanni EA, Rosenberg E, Zachariadis GA. Ultrasound-assisted magnetic solid-phase extraction of polycyclic aromatic hydrocarbons and nitrated polycyclic aromatic hydrocarbons from water samples with a magnetic polyaniline modified graphene oxide nanocomposite. Journal of Chromatography A. 2021 May 1645: 462104. DOI: https://doi.org/10.1016/j.chroma.2021.462104
Maria Claro A., Dias IKR, Fontes ML, Colturato VMM, Lima LR, Sávio LB, Berto GL, Arantes V, Barud HS. Bacterial cellulose nanocrystals obtained through enzymatic and acidic routes: A comparative study of their main properties and in vitro biological responses. Carbohydrate Research. 2024 Apr 539: 109104. DOI: https://doi.org/10.1016/j.carres.2024.109104
Mautner A. Nanocellulose water treatment membranes and filters: a review. Polymer International. 2020 Feb 69:741-751. DOI: https://doi.org/10.1002/pi.5993
Pampanin DM, Sydnes MO. Polycyclic aromatic hydrocarbons a constituent of petroleum: presence and influence in the aquatic environment. In Hydrocarbon 2013. InTech, Rijeka, Croatia. DOI: https://doi.org/10.5772/48176
PETROBRAS "Relatório Anual de Monitoramento da Água Produzida Descartada em Plataformas" 2021 [12/05/2025]. Available from: Relatórios Anuais: transparência é fundamental | Petrobras
PETROBRAS 2022 [12/05/2025]. Available from: Monitoramento de Água Produzida | Comunicação Bacia de Santos (petrobras.com.br)
Ruiz-Palomero C, Soriano ML, Valcárcel M. Nanocellulose as analyte and analytical tool: Opportunities and challenges. TrAC-Trends in Analytical Chemistry. 2017 Feb 87:1-18. DOI: https://doi.org/10.1016/j.trac.2016.11.007
Šafaříková M, Šafařík I. Magnetic solid-phase extraction. Journal of Magnetism and Magnetic Materials. 1999 Ap 194:108-112. DOI: https://doi.org/10.1016/S0304-8853(98)00566-6
Sasaki T, Tanaka S. Adsorption behavior of some aromatic compounds on hydrophobic magnetite for magnetic separation. Journal of Hazardous Materials. 2011 Nov 196:327-334. DOI: https://doi.org/10.1016/j.jhazmat.2011.09.033
Soares APS, Marques MFV, Mothé MG. Green Composite Sorbents from Coffee Capsule Waste and Eucalyptus urograndis Holocellulose. Arabian Journal for Science and Engineering. 2024 Mar 14:4539-4553. DOI: https://doi.org/10.1007/s13369-025-10030-2
Song X, Li J, Xu S, Ying R, Ma J, Liao C, Liu D, Yu J, Chen L. Determination of 16 polycyclic aromatic hydrocarbons in seawater using molecularly imprinted solid-phase extraction coupled with gas chromatography-mass spectrometry. Talanta. 2012 sep 99:75-8. DOI: https://doi.org/10.1016/j.talanta.2012.04.065
Sultanova NG, Kasarova SN, Nikolov ID. Characterization of optical properties of optical polymers. Optical and Quantum Electronics. 2013 Sep 45:221-232. DOI: https://doi.org/10.1007/s11082-012-9616-6
Venkatesan A, Wankat PC. Produced water desalination: An exploratory study. Desalination. 2017 Feb 404:328-340. DOI: https://doi.org/10.1016/j.desal.2016.11.013
WHO – World Health Organization "Water, Sanitation, hygiene and Health" 2019 [12/05/2025]. Available from: https://www.who.int/publications/i/item/9789240013391
Yang X, Yin Y, Zong Y, Wan T, Liao X. Magnetic nanocomposite as sorbent for magnetic solid phase extraction coupled with high performance liquid

chromatography for determination of polycyclic aromatic hydrocarbons. Microchemical Journal. 2019 Mar 145:26-34. DOI: https://doi.org/10.1016/j.microc.2018.10.013
Yang J, Zhang X, Wang X, Wang H, Zhao J, Zhou Z, Du X, Lu X. In situ anchor of multi-walled carbon nanotubes into iron-based metal-organic frameworks for enhanced adsorption of polycyclic aromatic hydrocarbons by magnetic solid-phase extraction. Journal of Chromatography A. 2022 Oct 1681:463459. DOI: https://doi.org/10.1016/j.chroma.2022.463459
Yaping L, Qi L, Shen Y, Ma H. Facile preparation of surface-exchangeable core@shell iron oxide@gold nanoparticles for magnetic solid-phase extraction: Use of gold shell as the intermediate platform for versatile adsorbents with varying self-assembled monolayers. Analytica Chimica Acta. 2014 Feb 811:36-42. DOI: https://doi.org/10.1016/j.aca.2013.12.020
Zhang S, Du Z, Li G. Layer-by-Layer Fabrication of Chemical-Bonded Graphene Coating for Solid-Phase Microextraction. Analytical Chemistry. 2011 Aug. 83:7531-7541. DOI: https://doi.org/10.1021/ac201864f
Zhang A, Zhao S, Wang L, Yang X, Zhao Q, Fan J, Yuan X. Polycyclic aromatic hydrocarbons (PAHs) in seawater and sediments from the northern Liaodong Bay, China. Marine Pollution Bulletin. 2016 Dec 113:592-599. DOI: https://doi.org/10.1016/j.marpolbul.2016.09.005